JOURNAL OF Applied Polymer SCIENCE

Fabrication and Characterization of Poly(vinyl alcohol)/Graphene Oxide Nanofibrous Biocomposite Scaffolds

Y. Y. Qi,[1,2] Z. X. Tai,[1,3] D. F. Sun,[1,3] J. T. Chen,[1] H. B. Ma,[1,2] X. B. Yan,[1] B. Liu,[2] Q. J. Xue[1]

[1]State Key Laboratory of Solid Lubrication, Lanzhou Institute of Chemical Physics, Chinese Academy of Sciences, Lanzhou 730000, China

[2]School of Stomatology, Lanzhou University, Lanzhou 730000, China

[3]Graduate University of Chinese Academy of Sciences, Beijing 100080, China

Correspondence to: X. B. Yan (E-mail: xbyan@licp.cas.cn) and B. Liu (E-mail: liubkq@lzu.edu.cn)

ABSTRACT: Nanofibrous biocomposite scaffolds of poly(vinyl alcohol) (PVA) and graphene oxide (GO) were prepared by using electrospinning method. The microstructure, crystallinity, and morphology of the scaffolds were characterized through X-ray diffraction (XRD), Fourier transform infrared spectroscopy (FTIR), and scanning electron microscopy (SEM). The mechanical properties were investigated by tensile testing. Moreover, Mouse Osteoblastic Cells (MC3T3-E1) attachment and proliferation on the nanofibrous scaffolds were investigated by MTT [3-(4,5-dimeth-ylthiazol-2-yl)-2,5-diphenyl tetrazolium bromide] assay, SEM observation and fluorescence staining. XRD and FTIR results verify the presence of GO in the scaffolds. SEM images show the three-dimensional porous fibrous morphology, and the average diameter of the composite fibers decreases with increasing the content of GO. The mechanical properties of the scaffolds are altered by changing the content of GO as well. The tensile strength and elasticity modulus increase when the content of GO is lower than 1 wt %, but decrease when GO is up to 3 and 5 wt %. MC3T3-E1 cells attach and grow on the surfaces of the scaffolds, and the adding of GO do not affect the cells' viability. Also, MC3T3-E1 cells are likely to spread on the PVA/GO composite scaffolds. Above all, these unique features of the PVA/GO nanofibrous scaffolds prepared by electrospinning would open up a wide variety of future applications in bone tissue engineering and drug delivery systems. © 2012 Wiley Periodicals, Inc. J. Appl. Polym. Sci. 000: 000–000, 2012

KEYWORDS: poly(vinyl alcohol); graphene oxide; nanofiber; biocomposite; electrospinning

Received 3 August 2011; accepted 17 April 2012; published online
DOI: 10.1002/app.37924

INTRODUCTION

Scaffolds play a central role in tissue engineering research, they not only provide as structural support for specific cells but also provide as the templates to guide new tissue growth and construction.[1] Therefore, fabricating three-dimensional porous scaffolds with good biocompatibility and biodegradability is an important aspect of tissue engineering. Electrospinning is a new technology developed rapidly in recent years, especially in tissue engineering. The fibers produced by electrospinning have diameter in the range of few microns to nanometer scale by applying high electric fields, and they form scaffolds with high porosity, high degree of surface area and other benefits, which resemble the topographic features of the natural extra cellular matrix (ECM). So these scaffolds provide a favorable environment for growth of new tissues.[2–6]

PVA, as a synthetic polymer, is easily obtained, nontoxic, water-soluble, biocompatible, and biodegradable, and it has good fiber-forming, highly hydrophilic, and good mechanical properties. Thus, PVA has been widely used in biomedical field.[7–10] However, because PVA is weak in cellular affinity, it is often combined with other materials to be implants.[11,12]

Recently, composites of polymer and nanotube (CNT) have been extensively researched for their applications as biomedical materials.[13,14] The CNT incorporated scaffolds have good mechanical property and are useful for stimulating cell growth.[15,16] However, the metal catalysts used in the fabrication of CNTs are generally trapped inside the nanotubes,[17–19] which has potential negative effects on their cytotoxicity.[20] Also, less-than-ideal dispersion of CNTs and the intrinsic defects appeared in dispersion process can cause problems in fabricating composite materials

which limit their applications in tissue engineering fields.[21,22] It is expected to have a metal-free nanocarbon material that may enhance the mechanical properties and biocompatibility of polymer scaffolds.

Nowadays, graphene and its derivatives have attracted great research interest because of their unique physicochemical properties. They have potential applications in electronics, energy, composites and biomedical areas.[23–25] Graphene oxide (GO) is one of the most important graphene derivatives,[26] and it has high Young's modulus and hardness, excellent flexibility, and low cost compared with CNTs, which make it an effective reinforcement for composites.[27] For GO, there are a large number of hydrophilic groups on its surface, such as hydroxyl, carboxyl, and epoxy,[28–30] so it can be dispersed at the individual sheet level in water, which is an ideal solvent for both PVA and GO.[31–33] Also, these groups can form hydrogen bonds with the polyvinyl alcohol molecule chains that contain even more hydrophilic groups, which could enhance the interfacial adhesion between GO and PVA and the mechanical performance of the resulting PVA/GO composite.[34] Up to now, PVA/GO composite hydrogels and films have been prepared.[35–38] Liang et al.[36] prepared a kind of poly(vinyl alcohol) (PVA) film with graphene oxide (GO) using a simple water solution processing method. Efficient load transfer is found between the nanofiller graphene and matrix PVA and the mechanical properties of the graphene-based nanocomposite with molecule-level dispersion are significantly improved. Putz et al.[38] fabricated a highly ordered, homogeneous polymer film of layered graphene oxide using a vacuum-assisted self-assembly (VASA) technique, which has allowed for the recognition that hydrogen bonding plays a critical role in the mechanical properties of both pure graphene oxide and composite paper samples. In this paper, we used electrospinning technique to prepare PVA/GO scaffolds, and investigated their microstructures, mechanical and biocompatible properties. It is expected to obtain a kind of materials which would combine the advantages of PVA/GO composites and nanofibrous structure together. To our knowledge, this is the first preparation of nanofibrous PVA/GO scaffolds with different additions of GO. Moreover, to evaluate their ability to support cell growth and proliferation, cell attachment and proliferation on the as-prepared scaffolds were investigated by MTT assay, scanning electron microscopy (SEM) observation and fluorescence staining.

EXPERIMENTAL

Materials

PVA (M_W = 77,000, 98% hydrolyzed) was supplied by Sinopharm Chemical Reagent, China. Graphite powder (325 mesh) was purchased from Qingdao Huatai Tech, China. Triton X-100 was obtained from Beijing solarbio science Technology, China. Fetal bovine serum (FBS) was purchased from Hangzhou Sijiqing Biological Engineering Materials, China. Mouse Osteoblastic Cell (MC3T3-E1) line and Roswell Park Memorial Institute 1640 (RPMI 1640) medium were purchased from Lanzhou Shenggong Biomedical, China. Trypsin-EDTA solution and 3-(4,5-dimethylthiazol-2-yl)-2,5-diphenyltetrazolium bromide (MTT) were purchased from Sigma. Other reagents were commercially available and were of analytical reagent grade. All chemicals and solvents were used as received.

Preparation of PVA/GO Solution and Electrospinning

GO was prepared according to the method described by Hummer with a modification.[39,40] In a typical synthesis, graphite powder (3 g, 325 mesh) was put into an 80°C solution of concentrated H_2SO_4 (12 mL), $K_2S_2O_8$ (2.5 g), and P_2O_5 (2.5 g). The mixture was kept at 80°C for 4.5 h using a hotplate. Successively, the mixture was cooled to room temperature and diluted with 0.5 L H_2O and left overnight. Then, the mixture was filtered and washed with H_2O using a 0.45 μm millipore-filter to remove the residual acid. The product was dried under ambient condition. This preoxidized graphite was then subjected to oxidation by Hummers' method described as follows. Pretreated graphite powder was put into cold (0°C) concentrated H_2SO_4 (120 mL). Then, $KMnO_4$ (15 g) was added gradually under stirring and the temperature of the mixture was kept to be below 20°C by cooling. Successively, the mixture was stirred at 35°C for 2 h, and then carefully diluted with 250 mL of H_2O. After that, the mixture was stirred for 2 h, and then additional 0.7 L of H_2O was added. Shortly, 20 mL of 30% H_2O_2 was added to the mixture. The resulting brilliant-yellow mixture was filtered and washed with 10 wt % HCl aqueous solution (1 L) to remove metal ions followed by washed repeatedly with H_2O to remove the acid until the pH of the filtrate was neutral. The GO slurry was dried in a vacuum oven at 60°C and purified by dialysis for one week. The synthesis procedure for a typical well-dispersed PVA/GO solution with GO loading of 1 wt % was as follows: GO (8 mg) was added to distilled water (9.2 mL) and then sonicated for 1 h. PVA (0.8 g) was dissolved in the GO aqueous dispersion and the mixture was stirred at 90°C for 4 h to obtain a homogeneous suspension, then it was cooled to room temperature. After that, Triton X-100 (0.3 wt %) was added to this suspension and sonicated for another 30 min. Here, Triton X-100 as a surfactant was used to decrease the surface tension of the suspension. The final suspension was electrospun at a constant voltage of 15 kV to produce nanofibers with a needle having an inner diameter of 0.6 mm and a feeding rate of 0.5 mL/h using a syringe pump. An aluminum collector connected to the ground was placed 10 cm from the tip of the needle to obtain nanofibrous scaffolds. A series of GO/PVA nanofibrous scaffolds with GO loading of 0, 0.5, 1, 3, and 5 wt % were prepared by the same procedure. The scaffolds were then dried overnight at 60°C under vacuum.

When an electrospun PVA scaffold is immersed in water, the scaffold shrinks and becomes transparent and gelatinous. For the purpose of cell culture on the nanofibrous scaffolds, the electrospun PVA/GO scaffolds were stabilized by simple soaking in methanol for 24 h, then dried and sterilized before cell seeding.

Morphological and Structural Characterizations

Transmission electron microscopy (TEM, JEOL, JEM-2010) was employed to investigate the morphology of as-prepared GO, using an accelerating voltage of 200 kV. TEM was also used to observe the morphology of the electrospun nanoscaffolds. XPS measurement of the GO was performed on a Perkin-Elmer

PHI-5702 multifunctional X-ray photoelectron spectroscope (Physical Electronics, USA), using Al-Kα radiation (photon energy 1476.6 eV) as the excitation source and the binding energy of Au (Au $4f_{7/2}$: 84.00 eV) as the reference. The electrospun nanoscaffolds were sputtering-coated with gold, to observe their images under field emission scanning electron microscope (FESEM, JEOL, JSM 6701F). The diameters of the resulting nanofibers were analyzed using Software Image. The crystallographic structure of the samples was determined by a powder X-ray diffraction system (XRD, Philips X' Pert Pro) equipped with CuKa radiation ($k = 0.15406$ nm). The diffraction angle was varied from 10° to 80°. Fourier transform infrared (FTIR, Bruker IFS66V) spectra were recorded using the flakes of samples pressed with KBr powders which was dried at 70°C to reduce the effect of the water molecules. The test range is between 4000 and 1000 cm^{-1}.

Mechanical Characterization

Tensile strength is the force per unit width of test specimen. An elastic modulus is defined as the slope of its stress–strain curve in the elastic deformation region.

Mechanical properties of the PVA and PVA/GO composite nanoscaffolds were measured by a universal testing machine (AGS-X5kN, Shimadzu Corporation). All the samples were cut into strips of 20 mm×4 mm×0.1 mm with a razor blade. The tensile tests were performed in a controlled velocity of clamps of 10 mm/min at room temperature. At least five samples were tested for each type of electrospun nanoscaffolds.

Characterization of *In Vitro* Biocompatibility

Cell Culture and Seeding. Mouse Osteoblastic Cells (MC3T3-E1) exhibit a developmental sequence similar to osteoblasts in bone tissue, namely, proliferation of undifferentiated osteoblast precursors followed by postmitotic expression of differentiated osteoblast phenotype. MC3T3-E1 cells were cultured in Roswell Park Memorial Institute 1640 (RPMI 1640) medium containing 10% fetal bovine serum, 50 U/mL penicillin and 50 U/mL streptomycin. The medium was replaced every 3 days and cultures were incubated in a cell culture incubator at 37°C with 5% CO_2. After reaching about 80% confluence, the cells were detached by 0.05% trypsin. A density of 10^4 cells/mL were seeded in 24-well plates for MTT assay and SEM observation after the electrospun nanoscaffolds were sterilized by ultraviolet irradiation for 2 h, and a density of 10^5 cells/mL for fluorescence staining observation.

MTT Assay. MTT assay is a cytotoxicity test method by evaluating the number of living cells and the strength to living cells metabolism. The toxicity of PVA and PVA/GO nanofibrous scaffolds to cell viability was evaluated using MTT assay (ISO10993-5 standard test method). After 1, 2, and 4 days of culture, the cell viability was evaluated by MTT assay, which was indicated by the reduction of MTT into a formazan dye by living cells. MTT solution (100 μL) at 5 mg/mL in phosphate buffered saline (PBS) was added to each well and incubated for 4 h under the same conditions described. After removal of the medium, the converted dye was dissolved in 750 μL/well dimethyl sulfoxide. Solution (150 μL) of each sample was transferred to a 96-well plate. Absorbance of converted dye was measured at a wavelength of 490 nm using an ELISA plate reader.

SEM Observation. After 1, 2, and 4 days of culture, the scaffolds were rinsed twice with PBS to remove nonadherent cells and subsequently fixed with 3% glutaraldehyde at 4°C for 4 h. After that, the samples were dehydrated through a series of graded ethanol solutions and air-dried overnight. Dry cellular constructs were sputtered with gold and observed by SEM (JSM-5600LV).

Fluorescence Staining Observation. After the same time intervals with above, cells were dehydrated through absolute ethyl alcohol, then the samples were stained with Acridine Orange (AO), which was cleaved to yield a green fluorescent product by metabolically active cells. The density of the cells which adhered on each scaffold was measured from randomly selected views of each film observed at 100-fold magnification with a fluorescence microscopy (Olympus BX51).

RESULTS AND DISCUSSION

Characterization of GO

As shown in Figure 1(a), as-prepared GO sheets are nearly transparent under electron irradiation, indicating the GO sheets are quite thin. As shown in Figure 1(b), the C1s XPS spectrum of GO indicates the presence of four components: the C in C═C bonds (284.5 eV), the C in C─O bonds (286.6 eV), the C in C═O bonds (287.7 eV), and the C in O─C═O bonds (288.7 eV). It indicates the considerable degree of the oxidation existing in GO material. The existence of the oxygen functionalized groups results in the hydrophilic nature of GO.

Morphology of the Scaffolds

The morphology of electrospun fibers is controlled by various parameters such as applied voltage, solution flow rate, distance between capillary and collector, and especially the concentration and surface tension of solution.[41,42] In our experiment, we routinely proceed electrospinning without additives, and only sporadic electrospraying of droplets is observed. To facilitate the electrospinning of PVA, a small amount of Triton X-100, a nonionic surfactant, was used to lower the surface tension of the PVA solution and increase its spin-ability.[43] Figure 2(a) shows a typical SEM image of the pure PVA nanofibers with the diameter in the range of 300–500 nm, which were electrospun from an 8 wt % PVA aqueous solution. Figure 2(b–e) show the SEM images of the PVA/GO composite nanofibers. As the images show, the composite nanofibers exhibit random fibrous morphology and interconnected porous structure, and the fibers had a majority of the diameters in the lower range of 50–300 nm. Compare with the pure PVA, the diameter of the PVA/GO composite scaffolds decreases, generally, at the same electrospinning conditions, if the electrical conductivity of electrospinning precursor solution is higher, the diameter of electrospun polymer fiber is thinner. In our system, the conductivity of the electrospinning solutions increases after adding GO, which is the main reason. In addition, wettability of PVA and GO could also be important factor. Moreover, as shown in Figure 2(e), some bead-like defects appear along the fibers, which indicates that the content of GO may be a critical factor to determine the

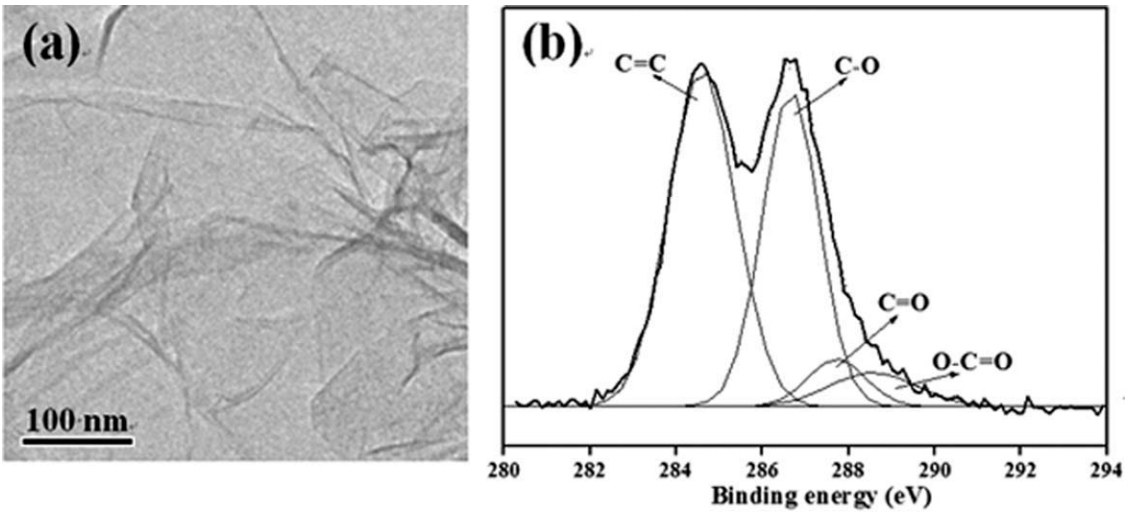

Figure 1. Characterization of GO sheets: (a) TEM image and (b) C1s XPS spectrum.

overall morphology of composite nanofibers. It is deduced that GO sheets tend to form aggregation when the content is above 3 wt %, which causes poor spin-ability of the solution.

Figure 3(a) shows the TEM image of electrospun PVA nanofibers, we found fibrous morphologies with uniform diameters. As shown in Figure 3(b,c), PVA/GO nanofibers had morphologies similar to the electrospun PVA nanofibers, and the added GO altered the morphology in some degree, whereas PVA/GO nanofibers with higher GO concent of 5 wt % showed micron size beads incorporated in nanofibers, unlike PVA/GO nanofibers with low GO content of 1 wt %, which had smooth fibrous morphology. We concluded that electrospun PVA/GO nanoscaffold with 1 wt % content of GO exhibited a noticeably smooth surface due to GO encapsulation, which reflected uniform distribution of GO in the PVA nanofibers.

XRD Investigation

XRD was used to investigate the crystallinity nature of pure PVA and PVA/GO (1,5 wt %) nanofibrous scaffolds and the corresponding XRD patterns are presented in Figure 4. From Figure 4, it can be observed that there is a diffraction peak located at 19.5°, which indicates the semi-crytalline nature of PVA and the lateral order structure of its molecular chain.[44] For the powdery GO sample, Figure 4(d) displays a strong (002) diffraction peak at 10.9°, corresponding to a *c*-axis spacing of 0.81 nm. As the GO sheets were added in the PVA fibers, the diffraction peak of the resulting PVA/GO scaffolds at 2θ =

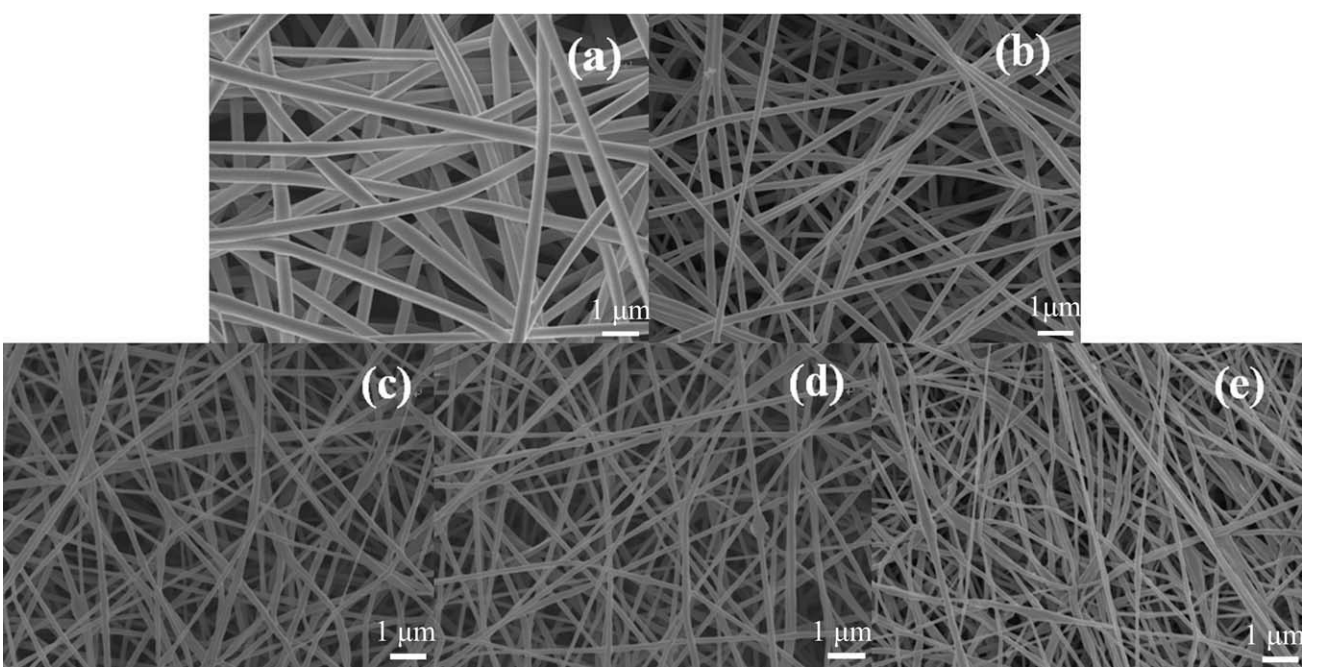

Figure 2. SEM images of electrospun fibrous scaffolds: (a) PVA, (b) PVA/GO (0.5 wt %), (c) PVA/GO (1 wt %), (d) PVA/GO (3 wt %), and (e) PVA/GO (5 wt %).

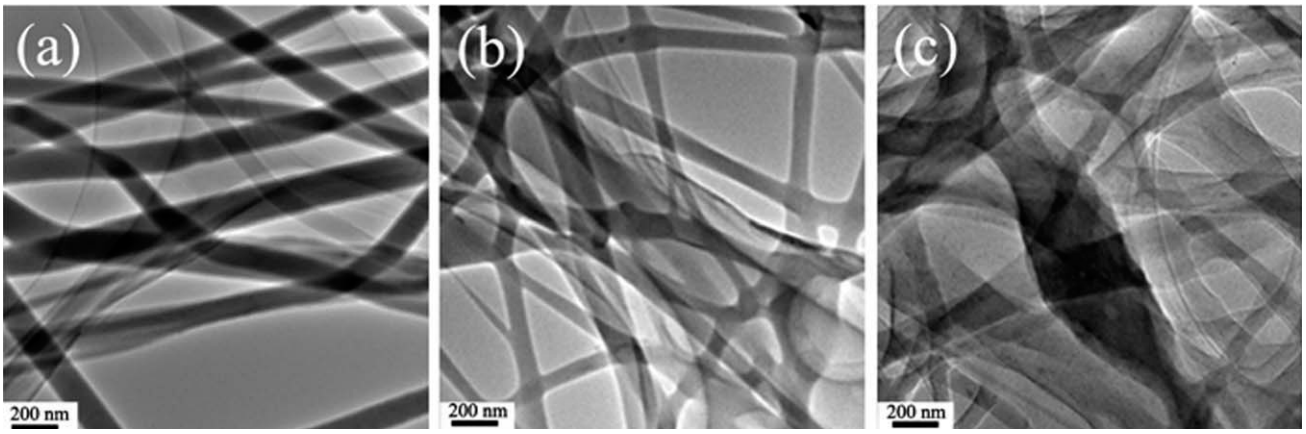

Figure 3. TEM images of electrospun fibrous scaffolds: (a) PVA, (b) PVA/GO (1 wt %), (c) PVA/GO (5 wt %).

19.5° becomes weaker which implies that the crystallization of PVA is deteriorated [Figure 4(b,c)]. It should be mentioned that, as shown in Figure 4(b,c), there is no diffraction peak attributed to GO phase in the XRD pattern of PVA/GO composite scaffold. It may be due to the relatively low content of GO in PVA matrix and exfoliation of GO.[45] In addition, van der Waals' forces and hydrogen bonds could be generated between PVA molecules and GO sheets,[46] as a result of strong interaction between them. This interaction would also affect the pristine crystallinity of GO sheets.

FTIR Investigation

FTIR spectroscopy is a fast and sensitive method for detecting various chemical bonds in materials. The FTIR spectra of pure PVA and PVA/GO (5 wt %) composite scaffolds are shown in Figure 5. In the IR spectrum of PVA [Figure 5(a)], the characteristic bands present in the 2800–3000 cm^{-1} and 1300−1500 cm^{-1} are due to the stretching and deformation vibrations of methyl/methylene/methine (CH_3/CH_2/CH). The intense band at 3100−3600 cm^{-1} is attributed to hydroxyl groups in each polymeric unit. Figure 5(b) shows the IR spectrum of PVA/GO (5 wt %) composite but no obvious change has been found compared with that of pure PVA. For GO [Figure 5(c)], the peaks at 3450, 1720, 1600, 1400, and 1100 cm^{-1} are assigned to the —OH stretching vibrations, C=O stretching vibrations in carboxylic acid, skeletal vibrations of unoxidized graphitic domains, O—H deformations of the C—OH groups and C—O stretching vibrations, respectively.

Mechanical properties

The mechanical properties of the PVA and PVA/GO scaffolds were evaluated by the tensile test. The variations of the tensile strength and the elasticity modulus as a function of GO content are showed in Figure 6. The tensile strength of the PVA/GO scaffolds increases with increasing the content of GO up to 1 wt %. For the PVA/GO scaffold with 1 wt % GO addition, the tensile strength is 4.6 MPa which is 21% higher than that of pure PVA scaffold. The increase in tensile strength is attributed to the nanometer-level dispersion of GO sheets in the polymer scaffolds. However, when the content of GO further increases, the tensile strength of the PVA/GO scaffolds gradually decreases.

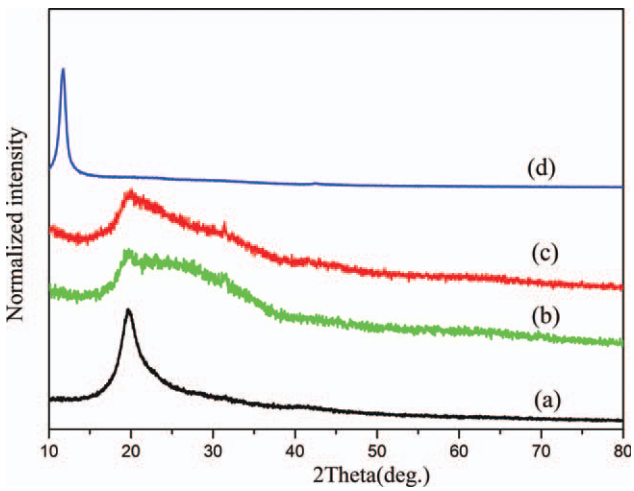

Figure 4. XRD patterns of electrospun fibrous scaffolds: (a) PVA, (b) PVA/GO (1 wt %), (c) PVA/GO (5 wt %), and (d) powdery GO. [Color figure can be viewed in the online issue, which is available at wileyonlinelibrary.com.]

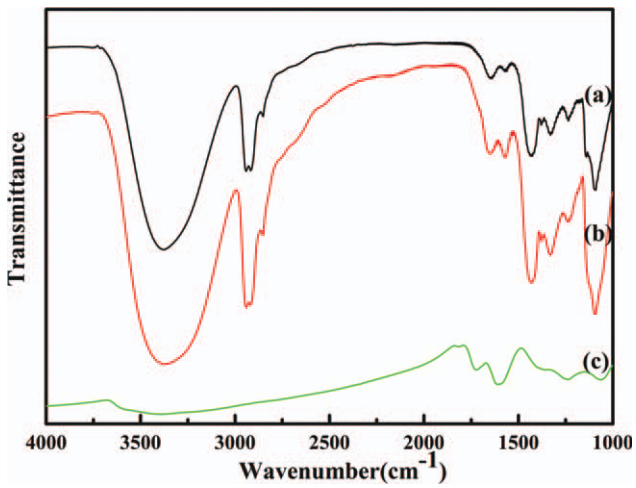

Figure 5. FTIR spectra of electrospun fibrous scaffolds: (a) PVA, (b) PVA/GO (5 wt %), and (c) powdery GO. [Color figure can be viewed in the online issue, which is available at wileyonlinelibrary.com.]

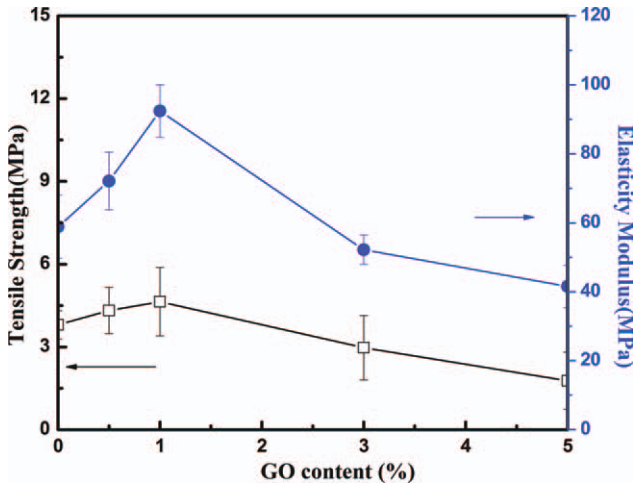

Figure 6. Tensile strength and elasticity modulus of the nanofibrous PVA and PVA/GO composite scaffolds with different GO contents. [Color figure can be viewed in the online issue, which is available at wileyonlinelibrary.com.]

For the PVA/GO scaffolds with 3 and 5 wt % GO additions, the values of their tensile strength are even lower than that of pure PVA scaffold. Similarly, the elastic modulus of the composite scaffolds has the similar variation with increasing the content of GO. These results are similar with other graphene/GO-reinforced polymer composites. Fan et al. observed that graphene-reinforced chitosan composites show improvement in the elastic modulus and hardness, but their values are irregular with the addition of graphene contents.[47] Wang et al. gave stress–strain curves of GO/polybenzimidazole composites, which indicate the tensile strength has a optimal value when GO content is 0.3 wt %, and too high or too low GO content would reduce the performance of materials.[48] To explain the mechanical properties of the PVA/GO composite scaffolds, for the composites with little GO content, GO sheets can be uniformly dispersed in the PVA matrix and favorable to load transfer from polymer matrix to GO, as a result of the enhancement of the tensile strength and the stiffness. However, when GO content is increased above a critical point, the PVA chains might be destroyed and the plastic deformation of the composites would reduce,[45] and GO sheets tend to aggregate as well. Also, From the XRD patterns, the broader peaks appeared in PVA/GO composites have shown the change in the structure of PVA which then could result in the changes in mechanical properties of the PVA/GO composite scaffolds. From above, it is concluded that the electrospun PVA/GO scaffolds are not able to obtain high tensile strength and elastic modulus, but they may be potential candidates for applications in lower or nonload bearing areas in tissue engineering.

Biocompatibility Test

MTT Assay. The viability of MC3T3-E1 cells cultured on different scaffolds within 4 days was shown in Figure 7. The increasing absorbance value indicates that osteoblasts on all scaffolds are able to convert the MTT into formazan product and continue to proliferate during the culture period. It can be seen that the viability of osteoblasts cultured on each scaffold increases with the increase of culture period, and the growth and proliferation of osteoblasts on the PVA/GO scaffolds tend to increase with increasing GO content. It can be definitely attributed to the excellent intrinsic biocompatibility and the hydrophilic nature of GO material.

SEM Observations. Osteoblasts with different culture period reflect the status of cell attachment and spread on a scaffold material. Osteoblasts were seeded on PVA and PVA/GO (1 wt %) scaffolds and cell images at different time intervals were observed by SEM (Figure 8). As images show [Figure 8(a,d)], after 24 h of incubation, cells exhibit obvious difference in morphology on the pure PVA and PVA/GO (1 wt %) composite scaffolds. On the pure PVA scaffold [Figure 8(a)], cells are round-shaped without extending and seem to have weak adhesion force with the substrate scaffold, while on PVA/GO composite scaffold [Figure 8(d)], cells adhered to the scaffold are close to bipolar-shaped with little extending. After 48 h of incubation, cells proliferate and growing close together on the pure PVA scaffold [Figure 8(b)], and the morphologies of the cells are mostly round shaped and still seem to have weak adhesion force with the substrate scaffold, while on the surfaces of the PVA/GO scaffold [Figure 8(e)], cells proliferate and spread on the surfaces of the composite scaffold, and the morphologies of the cells are bipolar shape with pseudopods out. After 96 h, cells become spreading and attaching on the surface of pure PVA scaffold and cells morphologies are close to bipolar shape [Figure 8(c)],while cells fully spread and exhibit bipolar morphology with numerous pseudopods attached on the surfaces of the PVA/GO scaffold [Figure 8(f)].

Additional, the unique nanofibrous structure of the electrospun PVA and PVA/GO are lost quickly when immersed in water. PVA can be chemically cross-linked with a variety of substances including glutaraldehyde, acetylaldehyde, or formaldehyde. Methanol treatment is used to stabilize the electrospun fibers to avoid introducing reactive species that could compromise

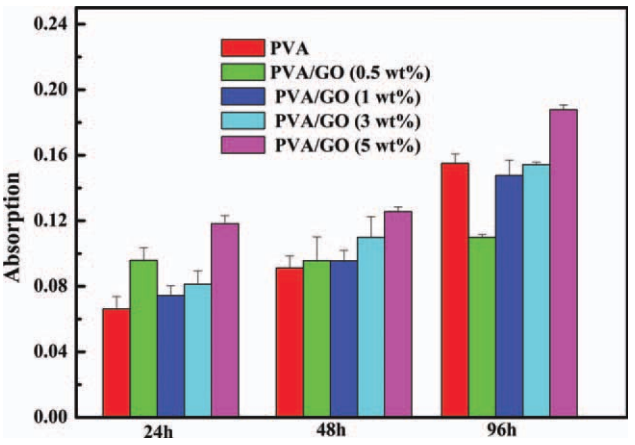

Figure 7. Formazan absorption (at 490 nm) in MTT assay was expressed as a measure of cell viability of MT3T3-E1cells seeded on electrospun PVA and PVA/GO composite scaffolds with different GO contents for 24, 48, and 96 h. [Color figure can be viewed in the online issue, which is available at wileyonlinelibrary.com.]

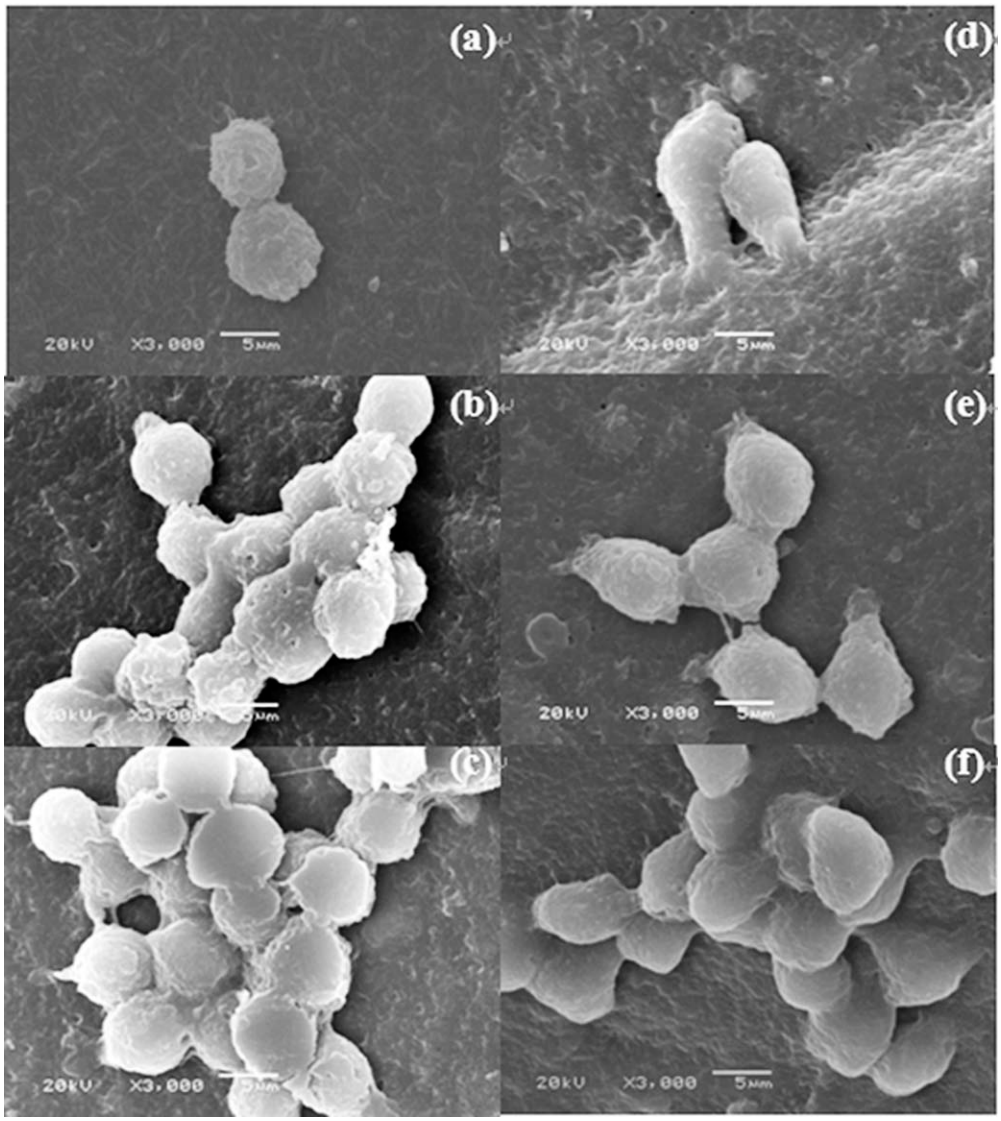

Figure 8. SEM images of MC3T3-E1 cells attached and spread on the surfaces of PVA and PVA/GO (1 wt %) scaffolds after (a and d) 24 h, (b and e) 48 h, and (c and f) 96 h of incubation.

biocompatibility from chemical cross-linking. Methanol treatment served to increase the degree of crystallinity, and hence the number of physical cross-links in the electrospun PVA fibers. This may occur by removal of residual water within the fibers by the alcohol, allowing PVA-water hydrogen bonding to be replaced by intermolecular polymer hydrogen bonding resulting in additional crystallization.[43,49] From SEM, although the scaffolds were stabilized by methanol, the morphological stability of the scaffolds was influenced by their immersing time in the cultures. It is indicates that osteoblasts have grown and proliferated well on the PVA/GO scaffold, and the added of GO is benefit for the cells' attaching and extending on the scaffold.

Fluorescence Staining Observation. Fluorescence microscope was used to examine the metabolically active of osteoblasts attached and proliferated on the pure PVA and PVA/GO(1 wt %) composite scaffolds after 24, 48, and 96 h of culture, respectively. After 24 h of culture, there are only a few cells on the scaffolds [Figure 9(a,d)]. By culturing for another 24 h, cells proliferate fast and are in good condition [Figure 9(b,e)]. After 96 h of culture, a subconfluent layer of cells is visualized [Figure 9(c,f)] on each scaffold, which suggests that the nanoporous surfaces are good for the growth and proliferation of osteoblasts. Scaffold properties play an active role in controlling the cell attachment and morphology,[50,51] and have a direct influence on intracellular responses. Cell adhesion and proliferation represent the initial phase of cell–scaffold communication that subsequently effect cell differentiation.[52,53] From the three phases, we can see cells' morphology on two kinds of scaffolds has slight difference, and osteoblasts are well-distributed with high density on the PVA/GO scaffold.

As we know, various carbon materials have been proven to be promising for biomedical applications such as tissue engineering and implants, in part because of their inherent biocompatibility. Also, GO and graphene have been proved to exhibit excellent

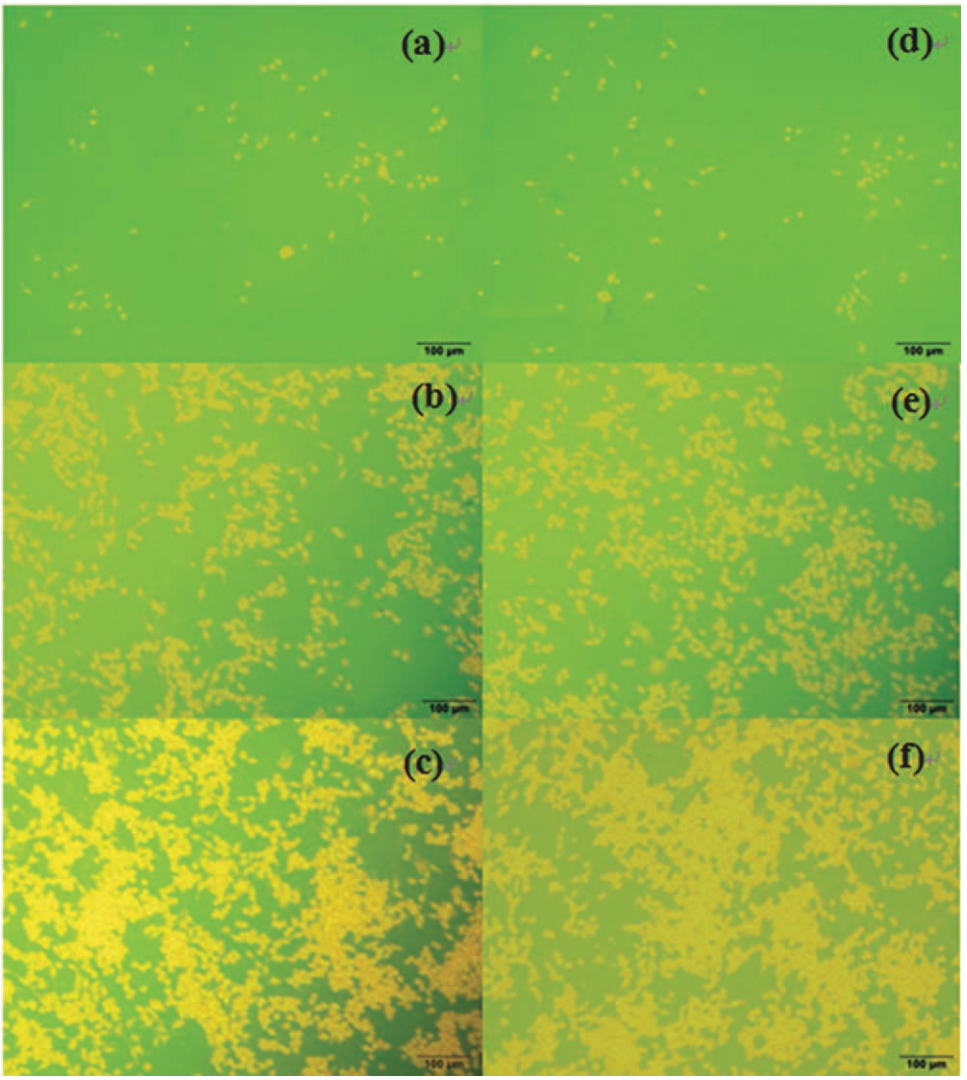

Figure 9. Fluorescence microscopic images of MC3T3-E1 cells grown and proliferated on the surfaces of PVA and PVA/GO (1 wt %) scaffolds after (a and d) 24 h, (b and e) 48 h, and (c and f) 96 h of incubation. [Color figure can be viewed in the online issue, which is available at wileyonlinelibrary.com.]

biocompatibility.[54] Fan et al. found that graphene/chitosan composites have good biocompatibility and cells can adhere and grow on the composite films as well as on pure chitosan film.[46] Liu et al. found that, because of the existence of the hydrophilic groups (carboxylic acid, hydroxyl and epoxide groups), GO sheets can promote the attachment and proliferation of human cells, especially retinal pigment epithelium (RPE) cells.[55] Due to their flat structure, GO nanosheets are expected to have even stronger interaction with the cellular membranes. Also, surface wettability is affected not only by surface chemistry but also by topographical parameters such as roughness and texture. Surface wettability of PVA and PVA/GO(1wt%) scaffolds may affect the proliferation of cells because the initial phase of attachment involves the physicochemical linkages between cells and surfaces through ionic forces or indirectly through an alteration in the adsorption of conditioning molecules e.g. proteins.[56] Therefore, we come to a conclusion that the addition of GO(1wt%) has no negative effect on the viability of osteoblast, and the preservation of biocompatibility for the PVA/GO composite scaffolds is attributed to the excellent intrinsic biocompatibility and the hydrophilic nature of GO.

CONCLUSIONS

GO sheets were successfully incorporated into PVA solutions to prepare nanofibrous biocomposite PVA/GO scaffolds by electrospinning technology. The effect of GO on the morphology, microstructure, mechanical properties and biocompatibility of the PVA/GO (1 wt %) composites were investigated in detail. The tensile strength and elasticity modulus increase when the content of GO is lower than 1 wt %, but decrease when GO is up to 3 and 5 wt %. The increased mechanical strengths of the PVA scaffold by the addition of GO are attributed to uniformly dispersion of GO phase and strong interactions between GO

and PVA. 1 wt % content of GO has no negative effect on the viability of osteoblasts, and the addition of GO is good for cells' adhering and spreading on the scaffolds. From the above, nanofibrous PVA/GO composite scaffolds prepared by electrospinning have potential use in lower or nonload bearing areas in tissue engineering and drug delivery systems.

The authors are grateful for the financial support by the National Natural Science Foundation of China, (Grant no.51005225) and the Top Hundred Talents Program of Chinese Academy of Sciences.

REFERENCES

1. Kim, B. S.; Mooney, D. J. *Trends Biotechnol.* **1998,** *16*, 224.
2. Liang, D.; Hsiao, B. S.; Chu, B. *Adv. Drug Deliv. Rev.* **2007,** *59*, 1392.
3. Pham, Q. P.; Sharma, U.; Mikos, A. G. *Tissue Eng.* **2006,** *12*, 1197.
4. Sill, T. J.; Recum, H. A. *Biomaterials* **2008,** *29*, 1989.
5. Barnes, C. P.; Sell, S. A.; Boland, E. D.; Simpson, D. G.; Bowlin, G. L. *Adv. Drug Deliv. Rev.* **2007,** *59*, 1413.
6. Ma, Z.; Kotaki, M.; Inai, R.; Ramakrishna, S. *Tissue Eng.* **2005,** *11*, 101.
7. Chen, R. S.; Chen, M. H.; Young, T. H. *Biomaterials* **2009,** *30*, 541.
8. Huang. R. Y. M.; Rhim, J. W. *Polym. Int.* **1993,** *30*, 123.
9. Gimenez, V.; Mantecon, A.; Cadiz, V. *J. Polym. Sci., Polym. Chem. Ed.* **1996,** *34*, 925.
10. Krumova, M.; Lopez, D.; Benavente, R.; Perena, J. M. *Polymer* **2000,** *41*, 9265.
11. Jang, J. H.; Castano, O.; Kim, H. W. *Adv. Drug Deliv. Rev.* **2009,** *61*, 1065.
12. Sill, T. J.; von Recum, H. A. *Biomaterials* **2008,** *29*, 1989.
13. Shi, X. F.; Hudson, J. L.; Spicer, P. P.; Tour, J. M.; Krishnamoorti, R.; Mikos, A. G. *Biomacromolecules* **2006,** *7*, 2237.
14. Veetil, J. V.; Ye, K. M. *Biotechnol. Prog.* **2009,** *25*, 709.
15. Sitharaman, B.; Shi, X.; Walboomers, X. F.; Liao, H.; Cuijpers, V., Wilson, L. J.; Mikos, A. G.; Jansen, J. A. *Bone* **2008,** *43*, 362.
16. Zanello, L. P.; Zhao, B.; Hu, H.; Haddon, R. C. *Nano. Lett.* **2006,** *6*, 562.
17. Correa-Duarte, M. A.; Wagner, N.; Rojas-Chapana, J.; Morsczeck, C.; Thie, M.; Giersig, M. *Nano. Lett.* **2004,** *4*, 2233.
18. Ge, C. C.; Lao, F.; Li, W.; Li, Y. F.; Chen, C. Y.; Qiu, Y.; Mao, X. Y.; Li, B.; Chai, Z. F.; Zhao, Y. L. *Anal. Chem.* **2008,** *80*, 9426.
19. Pumera, M. *Langmuir* **2007,** *23*, 6453.
20. Kolodiazhnyi, T.; Pumera, M. *Small* **2008,** *4*, 1476.
21. Badaire, S.; Poulin, P.; Maugey, M.; Zakri, C. *Langmuir* **2004,** *20*, 10367.
22. Dumitrica, T.; Hua, M.; Yakobson, B. I. *Proc Natl Acad Sci USA* **2006,** *103*, 6105.
23. Allen, M. J.; Tung, V. C.; Kaner, R. B. *Chem. Rev.* **2010,** *110*, 132.
24. Geim, A. K. *Science* **2009,** *324*, 1530.
25. Rao, C. N. R.; Sood, A. K.; Subrahmanyam, K. S.; Govindaraj, A. *Angew. Chem. Int. Ed.* **2009,** *48*, 7752.
26. Park, S.; Ruoff, R. S. *Nat. Nanotechnol.* **2009,** *4*, 217.
27. Chen, H. Q.; Mu]ller, M. B.; Gilmore, K. J.; Wallace, G. G.; Li, D. *Adv. Mater.* **2008,** *20*, 3557.
28. He, H.; Riedl, T.; Lerf, A.; Klinowski, J. *J. Phys. Chem.* **1996,** *100*, 19954.
29. Lerf, A.; He, H.; Forster, M.; Klinowski, J. *J. Phys. Chem. B* **1998,** *102*, 4477.
30. Hontoria-Lucas, C.; Lopez-Peinado, A. J.; Lopez-Gonzalez, J. de D.; Rojas-Cervantes, M. L.; Martin-Aranda, R. M. *Carbon* **1995,** *33*, 1585.
31. Stankovich, S.; Dikin, D. A.; Piner, R. D.; Kohlhaas, K. A.; Kleinhammes, A.; Jia, Y. Y.; Wu, Y.; Nguyen, S. T.; Ruoff, R. S. *Carbon* **2007,** *45*, 1558.
32. Schniepp, H. C.; Li, J. L.; McAllister, M. J.; Sai, H.; Herrera-Alonso, M.; Adamson, D. H.; Prud'homme, R. K.; Car, R.; Saville, D. A.; Aksay, I. A. *J. Phys. Chem. B* **2006,** *110*, 8535.
33. Cai, W. W.; Piner, R. D.; Stadermann, F. J.; Park, S.; Shaibat, M. A.; Ishii, Y.; Yang, D. X.; Velamakanni, A.; An, S. J.; Stoller, M.; An, J. H.; Chen, D. M.; Ruoff, R. S. *Science* **2008,** *321*, 1815.
34. Liu, L. Q.; Barber, A. H.; Nuriel, S.; Wagner, H. D. *Adv. Funct. Mater.* **2005,** *15*, 975.
35. Bai, H.; Li, C.; Wang, X. L.; Shi, G. Q. *Chem. Commun.* **2010,** *46*, 2376.
36. Liang, J.; Huang, Y.; Zhang, L.; Wang, Y.; Ma, Y. F.; Guo, T. Y.; Chen, Y. S. *Adv. Funct. Mater.* **2009,** *19*, 2297.
37. Bai, H.; Xu, Y. X.; Zhao, L.; Li, C.; Li, C.; Shi, G. Q. *Chem. Commun.* **2009,** *19*, 1667.
38. Putz, K. W.; Compton, O. C.; Palmeri, M. J.; Nguyen, S. T.; Brinson, L. C. *Adv. Funct. Mater.* **2010,** *20*, 3322.
39. Hummers, W. S.; Offeman, R. E. *J. Am. Chem. Soc.* **1958,** *80*, 1339.
40. Xu, Y.; Bai, H.; Lu, G.; Li, C.; Shi, G. *J. Am. Chem. Soc.* **2008,** *130*, 5856.
41. Deitzel, J. M.; Kleinmeyer, J.; Harris, D.; Tan, N. C. B. *Polymer* **2001,** *42*, 261.
42. Min, B. M.; You, Y.; Kim, J. M.; Lee, S. J.; Park, W.H. *Carbohydr. Polym.* **2004,** *57*, 285.
43. Li, Y.; Thomas, W. H.; Anthony, G. E.; Gary, L. B.; David, G. S.; Gary, E. W. *Chem. Mater.* **2003,** *15*, 1860.
44. Nishio, Y.; Manley, R. J. *Macromolecules* **1988,** *21*, 1270.
45. Bao, C.; Guo, Y.; Song, L.; Hu, Y. *J. Mater. Chem.* **2011,** *21*, 13942.
46. Kaczmarek, H.; Podgorski, A. *Polym. Degrad. Stab.* **2007,** *92*, 939.
47. Fan, H. L.; Wang, L. L.; Zhao, K. K.; Li, N.; Shi, Z. J.; Ge, Z. G.; Jin, Z. X. *Biomacromolecules* **2010,** *11*, 2345.
48. Wang, Y.; Shi, Z. X.; Fang, J. H.; Xu, H. J.; Yin, J. *Carbon* **2011,** *49*, 1199.

49. El-Refaie, K.; Fouad I, A. H.; Mohamed H. E. N.; Gary E. W. *Mater. Sci. Eng. A* **2007,** *459*, 390.

50. Miguel, A.; Correa, D.; Nicholas, W. *Nano. Lett.* **2004,** *4*, 2233.

51. Venugopal, J. R.; Low, S.; Choon, A. T.; Kumar, A. B.; Ramakrishna, S. *Artif. Organs* **2008,** *32*, 388.

52. von Recum, A. F.; van Kooten, T. G. *J. Biomater. Sci. Polym.* **1995,** *7*, 181.

53. Hutmacher, D. W. *Biomaterials* **2000,** *21*, 2529.

54. Yan, X. B.; Chen, J. T.; Yang, J.; Xue, Q. J.; Miele, P. *ACS Appl. Mater. Interfaces* **2010,** *2*, 2521.

55. Liu, Y.; Yu, D. S.; Zeng, C.; Miao, Z. C.; Dai, L. M. *Langmuir* **2010,** *26*, 6158.

56. Akasaka, T.; Yokoyama, A.; Matsuoka, M.; Hashimoto, T.; Watari, F. *Mater. Sci. Eng. C Mater. Biol. Appl.* **2010,** *30*, 391.